

Analysis of the Picard-Newton iteration for the incompressible Boussinesq equations

Elizabeth Hawkins*

September 2, 2024

Abstract

We study the Picard-Newton iteration for the incompressible Boussinesq equations, which is a two-step iteration resulting from the composition of the Picard and Newton iterations. We prove that this iterative method retains Newton's quadratic convergence but has less restrictive sufficient conditions for convergence than Newton and also is unconditionally stable under a small data condition. In this sense, Picard-Newton can be considered as a Newton iteration that is nonlinearly preconditioned with Picard. Our numerical tests illustrate this quadratic convergence and stability on benchmark problems. Furthermore, the tests show convergence for significantly higher Rayleigh number than both Picard and Newton, which illustrates the larger convergence basin of Picard-Newton that the theory predicts. We also introduce Anderson acceleration into the Picard step in our Picard-Newton numerical tests, and this enables convergence for even higher Rayleigh number.

1 Introduction

The incompressible Boussinesq equations are a multiphysics model of natural convection, and are commonly used to model flows with non-constant density or temperature. We consider this system on a finite connected domain $\Omega \subset \mathbb{R}^d$ ($d = 2, 3$) with $\partial\Omega = \Gamma_1 \cup \Gamma_2$, which is given by

$$\begin{cases} u \cdot \nabla u + \nabla p - \nu \Delta u &= f + R_i(0 \ T)^T \text{ in } \Omega, \\ \nabla \cdot u &= 0 \text{ in } \Omega, \\ u \cdot \nabla T - \kappa \Delta T &= g \text{ in } \Omega, \end{cases} \quad (1)$$

with boundary conditions

$$\begin{cases} u = 0 & \text{on } \partial\Omega, \\ T = 0 & \text{on } \Gamma_1, \\ \nabla T \cdot n = 0 & \text{on } \Gamma_2. \end{cases} \quad (2)$$

Here, u is the fluid velocity, p is the pressure, T is the temperature (or density), $\nu > 0$ is the kinematic viscosity of the fluid, $\kappa > 0$ is the thermal diffusivity, f is the external forcing term, and $R_i > 0$ is the Richardson number which accounts for the gravitational force and thermal expansion of the fluid.

The boundary conditions we state above are no-slip for velocity and mixed homogenous Dirichlet and homogenous Neumann for temperature (the latter of corresponds to perfect insulation), but our results are extendable to most common boundary conditions. Important physical constants are

*School of Mathematical and Statistical Sciences, Clemson University, Clemson, SC, 29364, evhawki@clemson.edu.

the Reynolds number Re , Prandtl number Pr which describes the ratio of kinematic viscosity and thermal diffusivity, and the Rayleigh number Ra :

$$Re = \nu^{-1} \quad Pr = \frac{\nu}{\kappa} \quad Ra = Ri \, Re^2 \, Pr.$$

The Picard iteration and Newton iteration are common iterative methods for solving the Boussinesq equations. The Picard iteration is given by

$$\begin{cases} u^k \cdot \nabla u^{k+1} + \nabla p^{k+1} - \nu \Delta u^{k+1} & = f + Ri(0 \, T^{k+1})^T, \\ \nabla \cdot u^{k+1} & = 0, \\ u^k \cdot \nabla T^{k+1} - \kappa \Delta T^{k+1} & = g, \end{cases} \quad (3)$$

with boundary conditions

$$\begin{cases} u^{k+1} = 0 & \text{on } \partial\Omega, \\ T^{k+1} = 0 & \text{on } \Gamma_1, \\ \nabla T^{k+1} \cdot n = 0 & \text{on } \Gamma_2, \end{cases} \quad (4)$$

and is known to admit stable solutions for any problem data. Furthermore provided the data satisfies a smallness condition, the solution to Picard is unique and the iteration converges linearly for any initial guess. Note that the system (3) decouples the equations because the heat transport equation is independent of velocity. While this all makes Picard very attractive with respect to efficiency at each iteration, the linear convergence is a potential drawback [15, 9, 24].

The Newton iteration for Boussinesq is given by

$$\begin{cases} u^{k+1} \cdot \nabla u^k + u^k \cdot \nabla u^{k+1} + \nabla p^{k+1} - \nu \Delta u^{k+1} & = f + Ri(0 \, T^{k+1})^T + u^k \cdot \nabla u^k, \\ \nabla \cdot u^{k+1} & = 0, \\ u^{k+1} \cdot \nabla T^k + u^k \cdot \nabla T^{k+1} - \kappa \Delta T^{k+1} & = g + u^k \cdot \nabla T^k, \end{cases} \quad (5)$$

with boundary conditions (4). This iteration will be shown in Section 2 to be well-posed and converge quadratically, but only for a very good initial guess and sufficiently small data (the sufficient conditions are more restrictive than for Picard). Newton is also more computationally expensive at each iteration, since it does not decouple and so one must solve fully coupled linear systems at each iteration. We note that it is common in fluid solvers to use Picard to find an initial guess for Newton by running Picard for several iterations.

The purpose of this paper is to consider the iteration defined by, at each step, first applying Picard and then applying Newton (called the Picard-Newton iteration). There are many other variations of utilizing both Picard and Newton together, which have improved efficiency and/or robustness of solvers for various problems [23, 14, 21, 16]. Our intent of combining the iterations in this way is to unite the speed of Newton with the stability and robustness of Picard. This method is simple to implement and we show it has an improved robustness compared to Newton but still converges quadratically. A similar improved robustness was shown both analytically and numerically in [18] for Picard-Newton applied to the Navier-Stokes equations.

We show herein analytically and numerically that the Picard-Newton iteration converges quadratically, with better convergence properties than Newton as well as improved stability. Due to our analytic results, the Picard-Newton iteration can be considered as the Newton iteration preconditioned with Picard, and thus fits a theme of recent and fundamentally important research called

nonlinear preconditioning [5, 13, 12]. We also show this method can be further improved using Anderson-acceleration (AA) in the Picard Step, which we call AAPicard-Newton.

This paper is arranged as follows. We provide analysis of the well-posedness, stability, and convergence of Picard and Newton iterations in section 2. While much of this is known, the proofs and results will allow for a better comparison and analysis of Picard-Newton. In section 3 we give analysis on the stability and convergence of Picard-Newton. Following this in section 4, we provide numerical results for Picard-Newton applied to some benchmark tests. Within this section we also combine Picard-Newton with AA and give numerical results that reveal this gives further improvement.

2 Preliminaries

Let $\Omega \subset \mathbb{R}^d$ ($d = 2$ or 3) be connected with boundary $\partial\Omega = \Gamma_1 \cup \Gamma_2$ where $meas(\Gamma_1 \cap \Gamma_2) = 0$. We denote the L^2 inner product and the L^2 norm on Ω as (\cdot, \cdot) and $\|\cdot\|$, respectively. We also denote the solution spaces for velocity, pressure, temperature, and divergence free velocity, as

$$\begin{aligned} X &= \{v \in H^1(\Omega) : v = 0 \text{ on } \partial\Omega\}, \\ Q &= \{q \in L^2(\Omega) : \int_{\Omega} q = 0\}, \\ D &= \{w \in H^1(\Omega) : w = 0 \text{ on } \Gamma_1 \text{ and } \nabla w \cdot n = 0 \text{ on } \Gamma_2\}, \\ V &= \{v \in X : (\nabla \cdot v, q) = 0 \ \forall q \in Q\}. \end{aligned}$$

Let X^* , V^* , and D^* be the dual spaces of X , V , and D , respectively. With slight abuse of notation, we also use (\cdot, \cdot) to denote the dual pairing of X and X^* , V and V^* , and D and D^* . Then for example, the dual norm of X is defined by

$$\|F\|_{X^*} := \sup_{z \in X} \frac{(F, z)}{\|z\|_X}.$$

We also recall the Poincaré inequality for $z \in X$ or D , given by

$$\|z\| \leq C_p \|\nabla z\|,$$

where $C_p > 0$ is a constant depending only on the size of the domain Ω .

Define the trilinear functionals $b : X \times X \times X \rightarrow \mathbb{R}$ and $\hat{b} : X \times D \times D \rightarrow \mathbb{R}$ by :

$$\begin{aligned} b(u, v, w) &:= (u \cdot \nabla v, w) + \frac{1}{2}((\nabla \cdot u)v, w), \\ \hat{b}(u, v, w) &:= (u \cdot \nabla s, t) + \frac{1}{2}((\nabla \cdot u)s, t). \end{aligned}$$

Then $b(u, v, w)$ and $\hat{b}(u, s, t)$ are skew-symmetric, i.e.,

$$b(u, v, v) = 0 \text{ and } \hat{b}(u, s, s) = 0.$$

Furthermore, if u is divergence free, then $b(u, v, w) = (u \cdot \nabla v, w)$, and thus $(u \cdot \nabla v, v) = 0$. A well known bound for b and \hat{b} that is used herein is [11]: $\forall u, v, w \in X, s, t \in D, \exists C_s > 0$ depending only on $|\Omega|$ such that

$$|b(u, v, w)| \leq C_s \|\nabla u\| \|\nabla v\| \|\nabla w\| \tag{6}$$

$$|\hat{b}(u, s, t)| \leq C_s \|\nabla u\| \|\nabla s\| \|\nabla t\| \tag{7}$$

The use of b and \hat{b} will allow for X, Q, D to be replaced by finite dimensional subspaces and have the exact same analysis of the paper hold.

2.1 Boussinesq equations background

The weak form of the Boussinesq equations is: Given $f \in X^*$ and $g \in D^*$, find $(u, p, T) \in (X, Q, D)$ satisfying $\forall (v, q, w) \in (X, Q, D)$,

$$\begin{cases} b(u, u, v) + (\nabla p, v) + \nu(\nabla u, \nabla v) &= (f, v) + R_i((0 \ T)^T, v), \\ (\nabla \cdot u, q) &= 0, \\ \hat{b}(u, T, w) + \kappa(\nabla T, \nabla w) &= (g, w). \end{cases}$$

The spaces (X, Q) satisfy an inf-sup condition, and thus the weak formulation is equivalently simplified using the solution space V : Find $(u, T) \in (V, D)$ satisfying $\forall (v, w) \in (V, D)$,

$$\begin{cases} b(u, u, v) + \nu(\nabla u, \nabla v) &= (f, v) + R_i((0 \ T)^T, v), \\ \hat{b}(u, T, w) + \kappa(\nabla T, \nabla w) &= (g, w). \end{cases} \quad (8)$$

Lemma 2.1. Any solution to the Boussinesq equations (8) satisfies the a priori estimate

$$\|\nabla T\| \leq \kappa^{-1} \|g\|_{D^*} =: M_2, \quad (9)$$

$$\|\nabla u\| \leq \nu^{-1} \|f\|_{V^*} + R_i C_p^2 \nu^{-1} M_2 =: M_1. \quad (10)$$

Proof. We let $v = u$ and $w = T$ in (8) then using skew-symmetry gives us

$$\begin{cases} \nu \|\nabla u\|^2 = R_i((0 \ T)^T, u) + (f, u), \\ \kappa \|\nabla T\|^2 = (g, T). \end{cases} \quad (11)$$

We upper bound the right hand side terms using the dual space norms, Cauchy-Schwarz, and Poincaré, which yields

$$\begin{aligned} R_i((0 \ T)^T, u) &\leq C_p^2 R_i \|\nabla T\| \|\nabla u\|, \\ (f, u) &\leq \|f\|_{V^*} \|\nabla u\|, \\ (g, T) &\leq \|g\|_{D^*} \|\nabla T\|. \end{aligned}$$

Using these bounds in (11) and reducing provides us with

$$\begin{cases} \|\nabla u\| \leq \nu^{-1} \|f\|_{V^*} + R_i C_p^2 \nu^{-1} \|\nabla T\|, \\ \|\nabla T\| \leq \kappa^{-1} \|g\|_{D^*}, \end{cases}$$

and using the second of these bounds in the first,

$$\|\nabla u\| \leq \nu^{-1} \|f\|_{V^*} + R_i C_p^2 \nu^{-1} \kappa^{-1} \|g\|_{D^*}.$$

This proves the result. □

The proof gives the bounds (9) and (10) for T and u respectively, and will be used throughout the paper for solutions to the Boussinesq equations. These results are similar to those found in [3], and depending on how the problem is formulated (e.g. Richardson number $\neq 1$ or Prandtl number $\neq 1$), the constants can differ but the results are equivalent. It is known that (8) admits solutions for any $Ra > 0$ [3], and this can be proven in the same way as the steady Navier-Stokes existence proof using the Leray-Schauder theorem [11]. Uniqueness of (8), however, requires a smallness assumption on the data. Below is a sufficient condition on the problem data that produces uniqueness.

Lemma 2.2. Let $\alpha_1 = C_s \nu^{-1} M_1$ and $\alpha_2 = C_s \kappa^{-1} M_2$. If $C_p^2 \nu^{-1} R_i, \alpha_2 + \alpha_1 < 1$, then solutions to (8) are unique.

Proof. Supposing two solutions (u_1, T_1) and (u_2, T_2) to (8) exist, define $e_u = u_1 - u_2$ and $e_T = T_1 - T_2$. Now subtracting the systems with these two solutions gives $\forall v \in V, w \in D$,

$$\begin{cases} b(u_1, e_u, v) + b(e_u, u_2, v) + \nu(\nabla e_u, \nabla v) & = Ri((0 \ e_T)^T, v), \\ \hat{b}(u_1, e_T, w) + \hat{b}(e_u, T_2, w) + \kappa(\nabla e_T, \nabla w) & = 0. \end{cases}$$

Taking $v = e_u$ and $w = e_T$ vanishes two nonlinear terms and leaves

$$\begin{cases} \nu \|\nabla e_u\|^2 & = Ri((0 \ e_T)^T, e_u) - b(e_u, u_2, e_u) \\ & \leq C_p^2 R_i \|\nabla e_T\| \|\nabla e_u\| + C_s \|\nabla e_u\|^2 \|\nabla u_2\|, \\ \kappa \|\nabla e_T\|^2 & = -\hat{b}(e_u, T_2, e_T) \\ & \leq C_s \|\nabla T_2\| \|\nabla e_u\| \|\nabla e_T\|. \end{cases}$$

Next, using the bounds (10) and (9) and simplifying gives

$$\begin{cases} \|\nabla e_u\| & \leq C_p^2 \nu^{-1} R_i \|\nabla e_T\| + \alpha_1 \|\nabla e_u\|, \\ \|\nabla e_T\| & \leq \alpha_2 \|\nabla e_u\|. \end{cases} \quad (12)$$

Adding these and simplifying results in

$$(1 - \alpha_1 - \alpha_2) \|\nabla e_u\| + (1 - C_p^2 \nu^{-1} R_i) \|\nabla e_T\| \leq 0.$$

This provides the uniqueness of the velocity due to the assumption on the data. With this, uniqueness of the temperature follows immediately from the second bound in (12). \square

2.2 Picard iteration

The weak formulations for Picard for the Boussinesq system takes the form: Find $(u^{k+1}, T^{k+1}) \in V \times D$ satisfying $\forall (v, w) \in V \times D$,

$$\begin{cases} b(u^k, u^{k+1}, v) + \nu(\nabla u^{k+1}, \nabla v) & = (f, v) + R_i((0 \ T^{k+1})^T, v), \\ \hat{b}(u^k, T^{k+1}, w) + \kappa(\nabla T^{k+1}, \nabla w) & = (g, w). \end{cases} \quad (13)$$

Note that the Picard iteration decouples the temperature equation and thus solving (13) is a two-step process where one first solves a scalar convection-diffusion problem and then an Oseen problem. Effective preconditioners for these linear systems exist in the literature [2, 6, 8, 4].

Lemma 2.3. Any solution to the Picard iteration for the Boussinesq equations satisfies the a priori estimate: for any $k = 1, 2, \dots$,

$$\begin{aligned} \|\nabla T^k\| & \leq M_2, \\ \|\nabla u^k\| & \leq M_1, \end{aligned}$$

Proof. These results are proved analogously to those of Lemma 2.1. \square

Lemma 2.4. The Picard iteration (13) with data satisfying $\min\{1 - \nu^{-1} \frac{C_p^2 R_i}{2}, 1 - \kappa^{-1} \frac{C_p^2 R_i}{2}\} > 0$, admits a unique solution.

Remark. Due to Lemma 2.3 and since (13) is linear, solution uniqueness can be proven immediately. In the finite dimensional case, this will also imply existence of solutions.

Proof. Let $Y = V \times D$ and at iteration $k + 1$ define $A : Y \times Y \rightarrow \mathbb{R}$ and $F : Y \rightarrow \mathbb{R}$ by

$$\begin{aligned} A((\hat{u}, \hat{T}), (v, w)) &:= b(u^k, \hat{u}, v) + \nu(\nabla \hat{u}, \nabla v) + \hat{b}(u^k, \hat{T}, w) + \kappa(\nabla \hat{T}, \nabla w) - R_i((0 \hat{T})^T, v), \\ F((v, w)) &= (f, v) + (g, w), \end{aligned}$$

so that the Picard iteration is given by $A((\hat{u}, \hat{T}), (v, w)) = F((v, w))$. Consider $A((\hat{u}, \hat{T}), (v, w))$. Using (6), Cauchy-Schwarz, and Young's inequality we lower bound the equation as

$$\begin{aligned} A((\hat{u}, \hat{T}), (\hat{u}, \hat{T})) &= b(u^k, \hat{u}, \hat{u}) + \nu \|\nabla \hat{u}\|^2 + \hat{b}(u^k, \hat{T}, \hat{T}) + \kappa \|\nabla \hat{T}\|^2 - R_i((0 \hat{T})^T, \hat{u}) \\ &\geq \nu \|\nabla \hat{u}\|^2 + \kappa \|\nabla \hat{T}\|^2 - \frac{C_p^2 R_i}{2} \|\nabla \hat{T}\|^2 - \frac{C_p^2 R_i}{2} \|\nabla \hat{u}\|^2 \\ &\geq \min\left\{\nu - \frac{C_p^2 R_i}{2}, \kappa - \frac{C_p^2 R_i}{2}\right\} \|(\hat{u}, \hat{T})\|_Y^2. \end{aligned}$$

Hence A is coercive. Continuity of A and F follow easily using the bounds and lemmas above. Thus Lax-Milgram applies and gives existence and uniqueness of (13). \square

We can now define the solution operator for the Picard iteration. Define $g_P : (V, D) \rightarrow (V, D)$ to be the solution operator for (13): $g_P(u^k, T^k) = (u^{k+1}, T^{k+1})$. Because the solutions to Picard are unique, this is a well defined operator.

Lemma 2.5. Consider the Picard iteration (13) with data satisfying $C_p^2 \nu^{-1} R_i < 1$ and $\alpha_1 + \alpha_2 < 1$. Then the iteration converges linearly with rate $\alpha_1 + \alpha_2$. In particular we have

$$\|\nabla(T - T^{k+1})\| \leq \alpha_2 \|\nabla(u - u^k)\|,$$

and

$$\|\nabla(u - u^{k+1})\| \leq (\alpha_1 + \alpha_2) \|\nabla(u - u^k)\|.$$

Remark. Note that the sufficient conditions for convergence of Picard are the same as the sufficient conditions for the uniqueness of solutions to the Boussinesq equations.

Proof. We subtract (8) from (13) and choose $v = e^{k+1}$ and $q = e_T^{k+1}$. Using skew-symmetry, vanishes two non-linear terms and leaves the equality

$$\begin{cases} b(e^k, u, e^{k+1}) + \nu \|\nabla e^{k+1}\|^2 &= R_i((0 e_T^{k+1})^T, e^{k+1}), \\ \hat{b}(e^k, T, e_T^{k+1}) + \kappa \|\nabla e_T^{k+1}\|^2 &= 0. \end{cases}$$

Next we use Cauchy-Schwarz, Poincaré, and (6) to upper bound these equations as

$$\begin{cases} \nu \|\nabla e^{k+1}\|^2 &\leq C_p^2 R_i \|\nabla e_T^{k+1}\| \|\nabla e^{k+1}\| + C_s \|\nabla e^k\| \|\nabla u\| \|\nabla e^{k+1}\|, \\ \kappa \|\nabla e_T^{k+1}\|^2 &\leq C_s \|\nabla e^k\| \|\nabla T\| \|\nabla e_T^{k+1}\|. \end{cases}$$

Then we reduce and apply Lemma 2.1 to get

$$\begin{cases} \|\nabla e^{k+1}\| &\leq C_p^2 \nu^{-1} R_i \|\nabla e_T^{k+1}\| + \alpha_1 \|\nabla e^k\|, \\ \|\nabla e_T^{k+1}\| &\leq \alpha_2 \|\nabla e^k\|. \end{cases}$$

this gives the bound

$$\|\nabla e_T^{k+1}\| \leq \alpha_2 \|\nabla e^k\|,$$

Adding the equations and reducing gives

$$\begin{aligned} \|\nabla e^{k+1}\| + (1 - C_p^2 R_i \nu^{-1}) \|\nabla e_T^{k+1}\|^2 &\leq C_s (\nu^{-1} \|\nabla u\| + \kappa^{-1} \|\nabla T\|) \|\nabla e^k\| \\ &\leq C_s (\nu^{-1} M_1 + \kappa^{-1} M_2) \|\nabla e^k\| \\ &\leq (\alpha_1 + \alpha_2) \|\nabla e^k\|. \end{aligned}$$

Finally, using the assumptions on the data finishes the proof. \square

2.3 Newton iteration

The weak formulation for the Newton iteration for the Boussinesq system takes the form: Find $(u^{k+1}, T^{k+1}) \in V \times D$ satisfying $\forall (v, w) \in V \times D$,

$$\begin{cases} b(u^{k+1}, u^k, v) + b(u^k, u^{k+1}, v) + \nu(\nabla u^{k+1}, \nabla v) &= (f, v) + R_i((0 \ T^{k+1})^T, v) \\ &\quad + b(u^k, u^k, v), \\ \hat{b}(u^{k+1}, T^k, w) + \hat{b}(u^k, T^{k+1}, w) + \kappa(\nabla T^{k+1}, \nabla w) &= (g, w) + \hat{b}(u^k, T^k, w). \end{cases} \quad (14)$$

Lemma 2.6. Consider the Newton iteration (14) with data and solutions satisfying

$$\begin{aligned} C_s \nu^{-1} \|\nabla(u^k - u)\| + \alpha_1 + C_s \nu^{-1} \|\nabla(T^k - T)\| + C_s \nu^{-1} M_2 + C_p^2 R_i &< 1, \\ \frac{C_s \kappa^{-1}}{4} \|\nabla(T^k - T)\| + \frac{\alpha_2}{4} + \frac{C_p^2 \kappa^{-1}}{4} R_i &< 1. \end{aligned}$$

Then there exists a unique solution to the iteration.

Proof. We proceed just like for Picard and will use Lax-Milgram. Let $Y = V \times D$ and at iteration $k + 1$ define $A : Y \times Y \rightarrow \mathbb{R}$ and $F : Y \rightarrow \mathbb{R}$ by

$$\begin{aligned} A((\hat{u}, \hat{T}), (v, w)) &:= b(\hat{u}, u^k, v) + b(u^k, \hat{u}, v) + \nu(\nabla \hat{u}, \nabla v) - R_i((0 \ \hat{T})^T, v) + \hat{b}(\hat{u}, T^k, w) + \hat{b}(u^k, \hat{T}, w), \\ &\quad + \kappa(\nabla \hat{T}, \nabla w) \\ F((v, w)) &= (f, v) + b(u^k, u^k, v) + (g, w) + \hat{b}(u^k, T^k, w). \end{aligned}$$

Then the Newton iteration is given by $A((\hat{u}, \hat{T}), (v, w)) = F((v, w))$. Continuity follows by applying (6), Poincaré, Cauchy-Schwarz, and Young's inequality

$$\begin{aligned} A((\hat{u}, \hat{T}), (v, w)) &= b(\hat{u}, u^k, v) + b(u^k, \hat{u}, v) + \nu(\nabla \hat{u}, \nabla v) - R_i((0 \ \hat{T})^T, v) \\ &\quad + \hat{b}(\hat{u}, T^k, w) + \hat{b}(u^k, \hat{T}, w) + \kappa(\nabla \hat{T}, \nabla w) \\ &\leq (2C_s \|\nabla u^k\| + \nu) \|\nabla \hat{u}\| \|\nabla v\| + C_p^2 R_i \|\nabla \hat{T}\| \|\nabla v\| \\ &\quad + C_s \|\nabla \hat{u}\| \|\nabla T^k\| \|\nabla w\| + (C_s \|\nabla u^k\| + \kappa) \|\nabla \hat{T}\| \|\nabla w\| \\ &\leq \sigma_{max} (\|\nabla \hat{u}\| + \|\nabla \hat{T}\|) (\|\nabla v\| + \|\nabla w\|) \\ &\leq \sigma_{max} \|(\hat{u}, \hat{T})\|_Y \|(v, w)\|_Y, \end{aligned}$$

where $\sigma_{max} = \max\{(2C_s \|\nabla u^k\| + \nu), C_p^2 R_i, C_s \|\nabla T^k\|, C_s \|\nabla u^k\| + \kappa\}$. The continuity of F is shown using the dual norms and (6) as

$$\begin{aligned} F((v, w)) &= (f, v) + b(u^k, u^k, v) + (g, w) + \hat{b}(u^k, T^k, w) \\ &\leq \|f\|_{V^*} \|v\| + C_s \|\nabla u^k\|^2 \|\nabla v\| + \|g\|_{D^*} \|\nabla w\| + C_s \|\nabla u^k\| \|\nabla T^k\| \|\nabla w\| \\ &\leq (\|f\|_{V^*} + C_s \|\nabla u^k\|^2 + \|g\|_{D^*} + C_s \|\nabla u^k\| \|\nabla T^k\|) \|(v, w)\|_Y. \end{aligned}$$

Next we show A is coercive, and this will require a restriction on the problem data. Here we use Cauchy-Schwarz and skew symmetry to lower bound A as

$$\begin{aligned}
A((\hat{u}, T), (\hat{u}, \hat{T})) &= b(\hat{u}, u^k, \hat{u}) + b(u^k, \hat{u}, \hat{u}) + \nu \|\nabla \hat{u}\|^2 + \hat{b}(\hat{u}, T^k, T) + b(u^k, \hat{T}, \hat{T}) + \kappa \|\nabla \hat{T}\|^2 \\
&\quad - R_i((0 \ \hat{T})^T, \hat{u}) \\
&\geq b(\hat{u}, u^k, \hat{u}) + \nu \|\nabla \hat{u}\|^2 + \hat{b}(\hat{u}, T^k, \hat{T}) + \kappa \|\nabla \hat{T}\|^2 - C_p^2 R_i \|\nabla \hat{T}\| \|\nabla \hat{u}\| \\
&\geq b(\hat{u}, u^k - u, \hat{u}) + b(\hat{u}, u, \hat{u}) + \nu \|\nabla \hat{u}\|^2 + \hat{b}(\hat{u}, T^k - T, \hat{T}) \\
&\quad + \hat{b}(\hat{u}, T, \hat{T}) + \kappa \|\nabla \hat{T}\|^2 - C_p^2 R_i \|\nabla \hat{T}\| \|\nabla \hat{u}\|.
\end{aligned}$$

Using the bound (6)

$$\begin{aligned}
b(\hat{u}, u^k - u, \hat{u}) &\geq -C_s \|\nabla \hat{u}\|^2 \|\nabla(u^k - u)\|, \\
\hat{b}(\hat{u}, u, \hat{u}) &\geq -C_s \|\nabla \hat{u}\|^2 \|\nabla u\| \geq -C_s M_1 \|\nabla \hat{u}\|^2, \\
b(\hat{u}, T^k - T, \hat{T}) &\geq -C_s \|\nabla u\| \|\nabla(T^k - T)\| \|\nabla \hat{T}\|, \\
\hat{b}(\hat{u}, T, \hat{T}) &\geq -C_s \|\nabla u\| \|\nabla T\| \|\nabla \hat{T}\| \geq -C_s M_2 \|\nabla \hat{u}\| \|\nabla \hat{T}\|,
\end{aligned}$$

Then we bound A using the same bounds as above to get

$$\begin{aligned}
A((\hat{u}, T), (\hat{u}, T)) &\geq (\nu - C_s \|\nabla(u^k - u)\| - C_s M_1) \|\nabla \hat{u}\|^2 \\
&\quad - (C_s \|\nabla(T^k - T)\| + C_s M_2 + C_p^2 R_i) \|\nabla u\| \|\nabla \hat{T}\| + \kappa \|\nabla \hat{T}\|^2 \\
&\geq (\nu - C_s \|\nabla(u^k - u)\| - C_s M_1) \|\nabla \hat{u}\|^2 \\
&\quad - (C_s \|\nabla(T^k - T)\| + C_s M_2 + C_p^2 R_i) \|\nabla \hat{u}\|^2 \\
&\quad - \left(\frac{C_s}{4} \|\nabla(T^k - T)\| + \frac{C_s}{4} M_2 + \frac{C_p^2}{4} R_i\right) \|\nabla \hat{T}\|^2 + \kappa \|\nabla \hat{T}\|^2 \\
&\geq (\nu - (C_s \|\nabla(u^k - u)\| + C_s M_1 + C_s \|\nabla(T^k - T)\| + C_s M_2 + C_p^2 R_i)) \|\nabla \hat{u}\|^2 \\
&\quad + \left(\kappa - \left(\frac{C_s}{4} \|\nabla(T^k - T)\| + \frac{C_s}{4} M_2 + \frac{C_p^2}{4} R_i\right)\right) \|\nabla \hat{T}\|^2 \\
&\geq \sigma_{min} \|(\hat{u}, \hat{T})\|_Y^2,
\end{aligned}$$

where

$$\begin{aligned}
\sigma_{min} &= \min\{(\nu - (C_s \|\nabla(u^k - u)\| + C_s M_1 + C_s \|\nabla(T^k - T)\| + C_s M_2 + C_p^2 R_i)), \\
&\quad (\kappa - (\frac{C_s}{4} \|\nabla(T^k - T)\| + \frac{C_s}{4} M_2 + \frac{C_p^2}{4} R_i))\}.
\end{aligned}$$

Hence A is coercive. Thus by Lax-Milgram, the Newton iteration (14) is well-posed. \square

With this well-posedness result, the solution operator of (14) defined by $g_N : (V, D) \rightarrow (V, D)$, $g_N(u^k, T^k) = (u^{k+1}, T^{k+1})$ is well-defined provided the data restrictions of Lemma 2.6 are satisfied. We note this is only a sufficient condition, and the Newton iteration for the Boussinesq equations (14) is believed to be well-posed on a much less restrictive set of parameters.

Lemma 2.7. Assume for any k that

$$\gamma_k := \alpha_1 + \alpha_2 + \nu^{-1} C_s \|\nabla(u - u^k)\| + \kappa^{-1} C_s \|\nabla(T - T^k)\| < 1,$$

and

$$C_p^2 \nu^{-1} R_i < 1.$$

Then the Newton iteration (5) converges quadratically for any u^k and T^k satisfying

$$C_s(1 - \max\{\gamma_k, C_p^2 R_i \nu^{-1}\})^{-1}(\kappa^{-1} + \nu^{-1})(\|\nabla(u - u^k)\| + \|\nabla(T - T^k)\|) < 1.$$

Proof. Let $e_T^{k+1} = T - T^{k+1}$ and $e^k = u - u^k$. We subtract (8) from (14), add and subtract $b(u, e^{k+1}, v)$ in the first equation and $\hat{b}(u^{k+1}, T, v)$ into the second, and set $v = e^{k+1}$ and $w = e_T^{k+1}$ to get

$$\begin{cases} b(e^{k+1}, e^k, e^{k+1}) & + b(e^{k+1}, u, e^{k+1}) + b(e^k, e^{k+1}, e^{k+1}) + b(u, e^{k+1}, e^{k+1}) + \nu \|\nabla e^{k+1}\|^2 \\ & = R_i((0 \ e_T^{k+1})^T, e^{k+1}) + b(e^k, e^k, e^{k+1}), \\ \hat{b}(e^{k+1}, e_T^k, e_T^{k+1}) & + \hat{b}(e^{k+1}, T, e_T^{k+1}) + \hat{b}(e^k, e_T^k, e_T^{k+1}) + \hat{b}(u, e_T^k, e_T^{k+1}) + \kappa \|\nabla e_T^{k+1}\|^2 \\ & = \hat{b}(e^k, e_T^k, e_T^{k+1}). \end{cases}$$

Next using skew symmetry, 4 terms in the system above vanish, leaving us with

$$\begin{cases} \nu \|\nabla e^{k+1}\|^2 & = R_i((0 \ e_T^{k+1})^T, e^{k+1}) + b(e^k, e^k, e^{k+1}) - b(e^{k+1}, e^k, e^{k+1}) - b(e^{k+1}, u, e^{k+1}), \\ \kappa \|\nabla e_T^{k+1}\|^2 & = \hat{b}(e^k, e_T^k, e_T^{k+1}) - \hat{b}(e^{k+1}, e_T^k, e_T^{k+1}) - \hat{b}(e^{k+1}, T, e_T^{k+1}). \end{cases}$$

We use the bound (6), Cauchy-Schwarz, Poincaré, and the stability bounds from Lemma 2.1 to upper bound the right hand side terms as

$$\begin{cases} \nu \|\nabla e^{k+1}\|^2 & \leq C_p^2 R_i \|\nabla e_T^{k+1}\| \|\nabla e^{k+1}\| + C_s \|\nabla e^k\|^2 \|\nabla e^{k+1}\| + C_s \|\nabla e^{k+1}\|^2 \|\nabla e^k\| + \nu \alpha_1 \|\nabla e^{k+1}\|^2, \\ \kappa \|\nabla e_T^{k+1}\|^2 & \leq C_s \|\nabla e^k\| \|\nabla e_T^k\| \|\nabla e_T^{k+1}\| + C_s \|\nabla e^{k+1}\| \|\nabla e_T^k\| \|\nabla e_T^{k+1}\| + \kappa \alpha_2 \|\nabla e^{k+1}\| \|\nabla e_T^{k+1}\|. \end{cases}$$

This reduces to

$$\begin{cases} (1 - \alpha_1 - \nu^{-1} C_s \|\nabla e^k\|) \|\nabla e^{k+1}\| & \leq C_p^2 \nu^{-1} R_i \|\nabla e_T^{k+1}\| + C_s \nu^{-1} \|\nabla e^k\|^2, \\ \|\nabla e_T^{k+1}\| & \leq \kappa^{-1} C_s \|\nabla e^k\| \|\nabla e_T^k\| + \kappa^{-1} C_s \|\nabla e^{k+1}\| \|\nabla e_T^k\| + \alpha_2 \|\nabla e^{k+1}\|. \end{cases} \quad (15)$$

Next we add the equations and reduce to get

$$\begin{aligned} (1 - \alpha_1 - \alpha_2 - \nu^{-1} C_s \|\nabla e^k\| - \kappa^{-1} C_s \|\nabla e_T^k\|) \|\nabla e^{k+1}\| & + (1 - C_p^2 \nu^{-1} R_i) \|\nabla e_T^{k+1}\| \\ & \leq C_s \nu^{-1} \|\nabla e^k\|^2 + \kappa^{-1} C_s \|\nabla e^k\| \|\nabla e_T^k\|, \\ & \leq C_s (\nu^{-1} + \kappa^{-1}) (\|\nabla e^k\| + \|\nabla e_T^k\|)^2. \end{aligned}$$

The left hand side is lower bounded as follows,

$$\begin{aligned} (1 - \max\{\gamma_k, C_p^2 R_i \nu^{-1}\}) (\|\nabla e^{k+1}\| + \|\nabla e_T^{k+1}\|) & \leq (1 - \alpha_1 - \alpha_2 - \nu^{-1} C_s \|\nabla e^k\| - \kappa^{-1} C_s \|\nabla e_T^k\|) \|\nabla e^{k+1}\| \\ & \quad + (1 - C_p^2 \nu^{-1} R_i) \|\nabla e_T^{k+1}\|. \end{aligned}$$

This reduces to,

$$\|\nabla e^{k+1}\| + \|\nabla e_T^{k+1}\| \leq C_s (1 - \max\{\gamma_k, C_p^2 R_i \nu^{-1}\})^{-1} (\kappa^{-1} + \nu^{-1}) (\|\nabla e^k\| + \|\nabla e_T^k\|)^2,$$

which completes the proof. \square

3 Analysis of the Picard-Newton iteration

In this section, we consider the Picard-Newton iteration for the Boussinesq system, then analyze its stability and convergence properties. We show that the incorporation of a Picard step stabilizes the Newton step and reduces the (sufficient conditions on) small data assumptions and closeness assumption of the initial guess.

Using the solution operators for Picard and Newton defined in the previous section, the Picard-Newton iteration is defined as $g_{PN} := g_N \circ g_P$ so that

$$g_{PN}(u^k, T^k) = g_N(g_P(u^k, p^k, T^k)) = (u^{k+1}, T^{k+1}).$$

Thus, the Picard-Newton iteration consists of two steps. The first step is the Picard step given by $g_P(u^k, T^k) = (\tilde{u}^{k+1}, \tilde{T}^{k+1})$ which is then followed by the Newton step given by $g_N(\tilde{u}^{k+1}, \tilde{T}^{k+1}) = (u^{k+1}, T^{k+1})$.

Algorithm 3.1. Given $(u^0, p^0, T^0) \in (X, Q, D)$.

for $k = 0, 1, 2, \dots$ **do**

Step 1: Solve for $(\tilde{u}^{k+1}, \tilde{T}^{k+1}) \in V \times D$ satisfying

$$\begin{cases} b(u^k, \tilde{u}^{k+1}, v) + \nu(\nabla \tilde{u}^{k+1}, \nabla v) &= (f, v) + R_i((0 \ \tilde{T}^{k+1})^T, v), \\ \hat{b}(u^k, \tilde{T}^{k+1}, w) + \kappa(\nabla \tilde{T}^{k+1}, \nabla w) &= (g, w). \end{cases} \quad (16)$$

Step 2: Solve for $(u^{k+1}, T^{k+1}) \in V \times D$ satisfying

$$\begin{cases} b(u^{k+1}, \tilde{u}^{k+1}, v) + b(\tilde{u}^{k+1}, u^{k+1}, v) + \nu(\nabla u^{k+1}, \nabla v) &= (f, v) + R_i((0 \ T^{k+1})^T, v) \\ &\quad + b(\tilde{u}^{k+1}, \tilde{u}^{k+1}, v), \\ \hat{b}(u^{k+1}, \tilde{T}^{k+1}, w) + \hat{b}(\tilde{u}^{k+1}, T^{k+1}, w) + \kappa(\nabla T^{k+1}, \nabla w) &= (g, w) + \hat{b}(\tilde{u}^{k+1}, \tilde{T}^{k+1}, w). \end{cases} \quad (17)$$

end for

Picard is known to be unconditionally stable, while Newton is not (and is consequently divergent for many Ra). Therefore it is intuitive that the stability of Picard will have a positive effect on the stability of Picard-Newton. Hence, we begin by analyzing the stability of Picard-Newton.

Theorem 3.2. *If $\alpha_1 + \alpha_2$, $\nu^{-1}R_i C_p^2 < 1$ the Picard-Newton iteration (16)-(17) is stable with*

$$(1 - \alpha_1 - \alpha_2)\|\nabla u^{k+1}\| + (1 - \nu^{-1}R_i C_p)\|\nabla T^{k+1}\| \leq M_2 + 2M_1.$$

Remark. The small data conditions for stability of Picard-Newton are the same as the uniqueness condition for the Boussinesq equations.

Proof. We begin by considering the stability bound resulting from the Picard step. This part of the proof follows analogously to Lemma 2.3 resulting in

$$\begin{cases} \|\nabla \tilde{u}^{k+1}\| &\leq M_1, \\ \|\nabla \tilde{T}^{k+1}\| &\leq M_2. \end{cases}$$

Next we consider (17) and choose $v = u^{k+1}$ and $w = T^{k+1}$. This gives

$$\begin{cases} \nu\|\nabla u^{k+1}\|^2 &= (f, u^{k+1}) + R_i((0 \ T^{k+1})^T, u^{k+1}) + b(\tilde{u}^{k+1}, \tilde{u}^{k+1}, u^{k+1}) - b(u^{k+1}, \tilde{u}^{k+1}, u^{k+1}), \\ \kappa\|\nabla T^{k+1}\|^2 &= (g, T^{k+1}) + \hat{b}(\tilde{u}^{k+1}, \tilde{T}^{k+1}, T^{k+1}) - \hat{b}(u^{k+1}, \tilde{T}^{k+1}, T^{k+1}). \end{cases}$$

We next use Cauchy-Schwarz, upper bound the trilinear term, use Poincaré, and reduce to get

$$\begin{cases} \nu \|\nabla u^{k+1}\| & \leq \|f\|_{V^*} + R_i C_p^2 \|\nabla T^{k+1}\| + C_s \|\nabla \tilde{u}^{k+1}\|^2 + C_s \|\nabla u^{k+1}\| \|\nabla \tilde{u}^{k+1}\|, \\ \kappa \|\nabla T^{k+1}\| & \leq \|g\|_{D^*} + C_s \|\nabla \tilde{u}^{k+1}\| \|\nabla \tilde{T}^{k+1}\| + C_s \|\nabla u^{k+1}\| \|\nabla \tilde{T}^{k+1}\|. \end{cases}$$

Using the stability bound for the Picard step and combining like terms

$$\begin{cases} (1 - \alpha_1) \|\nabla u^{k+1}\| & \leq \nu^{-1} \|f\|_{V^*} + \nu^{-1} R_i C_p^2 \|\nabla T^{k+1}\| + \alpha_1 M_1, \\ \|\nabla T^{k+1}\| & \leq \kappa^{-1} \|g\|_{D^*} + \alpha_2 M_1 + \alpha_2 \|\nabla u^{k+1}\|, \end{cases}$$

where $\alpha_1 = \nu^{-1} C_s M_1$ and $\alpha_2 = \kappa^{-1} C_s M_2$.

We add the equations and combine like terms to obtain

$$(1 - \alpha_1 - \alpha_2) \|\nabla u^{k+1}\| + (1 - \nu^{-1} R_i C_p) \|\nabla T^{k+1}\| \leq \nu^{-1} \|f\|_{V^*} + \kappa^{-1} \|g\|_{D^*} + (\alpha_1 + \alpha_2) M_1.$$

Using that $M_2 = \kappa^{-1} \|g\|_{D^*}$ and $M_1 = \nu^{-1} \|f\|_{V^*} + R_i C_p^2 \nu^{-1} M_2$ we can upper bound the left hand side to get the bound

$$(1 - \alpha_1 - \alpha_2) \|\nabla u^{k+1}\| + (1 - \nu^{-1} R_i C_p) \|\nabla T^{k+1}\| \leq M_2 + (\alpha_1 + \alpha_2 + 1) M_1, \quad \leq M_2 + 2M_1.$$

□

One way to understand the effect of Picard's stability on Newton is to consider the case when u^k does not satisfy the sufficient conditions for convergence of Newton. In this case, one would expect that the Newton step could produce solutions which are divergent. However this is not the case because of Picard's stability bound.

Picard-Newton is a two step method and so for clarity we split the error analysis into two theorems: a theorem for the error arising in the Picard step and a theorem for the iterations error after the Newton step. The analysis for the Picard step will follow very closely to the analysis for the usual Picard iteration and thereby includes the constants M_1 and M_2 that naturally arise in the analysis.

Theorem 3.3. *Assume $C_p^2 R_i \nu^{-1} < 1$. Then the Picard step (16) of the Picard-Newton iteration satisfies*

$$\|\nabla(u - \tilde{u}^{k+1})\| + (1 - R_i C_p^2 \nu^{-1}) \|\nabla(T - \tilde{T}^{k+1})\| \leq (\alpha_1 + \alpha_2) \|\nabla(u - u^k)\|.$$

In particular we have,

$$\|\nabla(T - \tilde{T}^{k+1})\| \leq \alpha_2 \|\nabla(u - u^k)\|, \quad (18)$$

and

$$\|\nabla(u - \tilde{u}^{k+1})\| \leq (\alpha_1 + \alpha_2) \|\nabla(u - u^k)\|. \quad (19)$$

Proof. This proof follows analogously to Lemma 2.5.

□

Note that the bounds above on $(u - \tilde{u}^{k+1})$ and $(T - \tilde{T}^{k+1})$ both depend upon $(u - u^k)$. This means the accuracy of \tilde{T}^{k+1} depends on the accuracy of u^k for the Picard step.

Theorem 3.4. Assume $R_i C_p^2 \nu^{-1} < 1$ and

$$\beta_k := \alpha_1 + \alpha_2 + C_s(\alpha_1 + \alpha_2)[\kappa^{-1} + \nu^{-1}]\|\nabla(u - u^k)\| < 1$$

for any k . Then the Picard-Newton iteration will converge quadratically for any u^k satisfying

$$(1 - \max\{\beta_k, R_i C_p^2 \nu^{-1}\})^{-1} C_s(\alpha_1 + \alpha_2)^2 (\nu^{-1} + \kappa^{-1}) \|\nabla(u - u^k)\| < 1.$$

Proof. We subtract (17) from (8), then add and subtract terms and we the skew symmetry of the trilinear terms to write

$$\begin{cases} b(e^{k+1}, \tilde{e}^{k+1}, e^{k+1}) + b(e^{k+1}, u, e^{k+1}) + \nu \|\nabla e^{k+1}\|^2 &= (R_i(0 e_T^{k+1})^T, e^{k+1}) + b(\tilde{e}^{k+1}, \tilde{e}^{k+1}, e^{k+1}), \\ \hat{b}(e^{k+1}, \tilde{e}_T^{k+1}, e_T^{k+1}) + \hat{b}(e^{k+1}, T, e_T^{k+1}) + \kappa \|\nabla e_T^{k+1}\|^2 &= \hat{b}(\tilde{e}^{k+1}, \tilde{e}_T^{k+1}, e_T^{k+1}), \end{cases}$$

where $e_T^{k+1} = T^{k+1} - T$ and $e^{k+1} = u^{k+1} - u$.

We now use the bounds from Lemma 2.1 to get the upper bounds

$$\begin{cases} \nu \|\nabla e^{k+1}\|^2 &\leq C_p^2 R_i \|\nabla e_T^{k+1}\| \|\nabla e^{k+1}\| + C_s \|\nabla \tilde{e}^{k+1}\|^2 \|\nabla e^{k+1}\| + C_s \|\nabla e^{k+1}\|^2 \|\nabla \tilde{e}^{k+1}\| + \alpha_1 \nu \|\nabla e^{k+1}\|^2, \\ \kappa \|\nabla e_T^{k+1}\|^2 &\leq C_s \|\nabla \tilde{e}^{k+1}\| \|\nabla \tilde{e}_T^{k+1}\| \|\nabla e_T^{k+1}\| + C_s \|\nabla e^{k+1}\| \|\nabla \tilde{e}_T^{k+1}\| \|\nabla e_T^{k+1}\| + \kappa \alpha_2 \|\nabla e^{k+1}\| \|\nabla e_T^{k+1}\|, \end{cases}$$

which reduces to

$$\begin{cases} (1 - \alpha_1) \|\nabla e^{k+1}\| &\leq C_p^2 \nu^{-1} R_i \|\nabla e_T^{k+1}\| + C_s \nu^{-1} \|\nabla \tilde{e}^{k+1}\|^2 + C_s \nu^{-1} \|\nabla e^{k+1}\| \|\nabla \tilde{e}^{k+1}\|, \\ \|\nabla e_T^{k+1}\| &\leq C_s \kappa^{-1} \|\nabla \tilde{e}^{k+1}\| \|\nabla \tilde{e}_T^{k+1}\| + C_s \kappa^{-1} \|\nabla e^{k+1}\| \|\nabla \tilde{e}_T^{k+1}\| + \alpha_2 \|\nabla e^{k+1}\|. \end{cases}$$

Next we continue bounding using (19) and (18) to obtain

$$\begin{cases} (1 - \alpha_1) \|\nabla e^{k+1}\| &\leq C_p^2 \nu^{-1} R_i \|\nabla e_T^{k+1}\| + C_s \nu^{-1} (\alpha_1 + \alpha_2)^2 \|\nabla e^k\|^2 + C_s \nu^{-1} (\alpha_1 + \alpha_2) \|\nabla e^{k+1}\| \|\nabla e^k\|, \\ \|\nabla e_T^{k+1}\| &\leq C_s \kappa^{-1} \alpha_2 (\alpha_1 + \alpha_2) \|\nabla e^k\|^2 + C_s \kappa^{-1} \alpha_2 \|\nabla e^{k+1}\| \|\nabla e^k\| + \alpha_2 \|\nabla e^{k+1}\|. \end{cases}$$

Adding the equations and reducing yields

$$\begin{aligned} (1 - \alpha_1 - \alpha_2 - C_s[\kappa^{-1} \alpha_2 + \nu^{-1}(\alpha_1 + \alpha_2)]) \|\nabla e^k\| \|\nabla e^{k+1}\| &+ (1 - C_p^2 \nu^{-1} R_i) \|\nabla e_T^{k+1}\| \\ &\leq C_s (\alpha_1 + \alpha_2) (\nu^{-1} (\alpha_1 + \alpha_2) + \kappa^{-1} \alpha_2) \|\nabla e^k\|^2 \\ &\leq C_s (\alpha_1 + \alpha_2)^2 (\nu^{-1} + \kappa^{-1}) \|\nabla e^k\|^2. \end{aligned}$$

We now lower bound the left hand side as

$$(1 - \max\{\beta_k, C_p^2 R_i \nu^{-1}\}) (\|\nabla e^{k+1}\| + \|\nabla e_T^{k+1}\|) \leq (1 - \alpha_1 - \alpha_2 - C_s[\kappa^{-1} \alpha_2 + \nu^{-1}(\alpha_1 + \alpha_2)]) \|\nabla e^k\| \|\nabla e^{k+1}\| + (1 - C_p^2 R_i \nu^{-1}) \|\nabla e_T^{k+1}\|,$$

and upper bound the right hand side to obtain

$$\|\nabla e^{k+1}\| + \|\nabla e_T^{k+1}\| \leq (1 - \max\{\beta_k, C_p^2 R_i \nu^{-1}\})^{-1} C_s (\alpha_1 + \alpha_2)^2 (\nu^{-1} + \kappa^{-1}) \|\nabla e^k\|^2.$$

□

We provide table 1 below for a more clear comparison of the sufficient conditions for Newton and Picard-Newton. First notice that the assumptions for Picard-Newton include similar terms, and in fact they both require $C_p^2 R_i \nu^{-1} < 1$. However, it is clear that Picard-Newton's assumptions are less restrictive as they do not include any assumptions on T , and the velocity term in β_k in Picard-Newton is scaled by $(\alpha_1 + \alpha_2)$ compared to Newton (note that this same condition ensures $(\alpha_1 + \alpha_2) < 1$). These weakened restrictions for Picard-Newton are due to the Picard step allowing u^k to control the error of T .

Similarly, the sufficient condition on the initial guess for convergence of Picard-Newton is scaled by $(\alpha_1 + \alpha_2)^2$ compared to Newton. Because another sufficient condition for Picard-Newton ensures that $\alpha_1 + \alpha_2 < 1$, this allows more u^k to satisfy the equation

$$C_s(1 - \max\{\beta_k, C_p^2 R_i \nu^{-1}\})^{-1}(\alpha_1 + \alpha_2)^2(\nu^{-1} + \kappa^{-1})\|\nabla(u - u^k)\| < 1.$$

However there is another important connection to be made between Picard and the sufficient conditions. If we consider just Picard, it is required for its convergence that $\alpha_1 + \alpha_2 < 1$. Then for Picard-Newton, α_1 and α_2 come from the error of the Picard step and appear in the sufficient conditions and assumptions of the method. This means that Picard-Newton's conditions for convergence are potentially being aided by Picard's convergence properties. Furthermore, recall that the assumption for uniqueness of solutions to Boussinesq equations includes $\alpha_1 + \alpha_2 < 1$. This further shows the assumption is reasonable and therefore Picard-Newton's sufficient conditions for convergence of Picard-Newton are improved when compared to Newton.

Sufficient conditions
Newton
$\gamma_k = \alpha_1 + \alpha_2 + \nu^{-1} C_s \ \nabla(u - u^k)\ + \kappa^{-1} C_s \ \nabla(T - T^k)\ < 1$ $C_p^2 \nu^{-1} R_i < 1$
$(1 - \max\{\gamma_k, C_p^2 R_i \nu^{-1}\})^{-1}(\kappa^{-1} + \nu^{-1})(\ \nabla(u - u^k)\ + \ \nabla(T - T^k)\) < 1$
Picard-Newton
$\beta_k = \alpha_1 + \alpha_2 + C_s(\alpha_1 + \alpha_2)[\kappa^{-1} + \nu^{-1}]\ \nabla(u - u^k)\ < 1$ $C_p^2 R_i \nu^{-1} < 1$
$(1 - \max\{\beta_k, C_p^2 R_i \nu^{-1}\})^{-1}(\alpha_1 + \alpha_2)^2(\nu^{-1} + \kappa^{-1})\ \nabla(u - u^k)\ < 1$

Table 1: Shown above is a comparison of sufficient conditions for Newton and Picard-Newton convergence.

4 Numerical Results

We give now numerical results for two test problems for Picard-Newton applied to the Boussinesq equations. We consider the Boussinesq system with $g = 0$, $f = 0$, $\nu = \kappa = 10^{-1}$, and Ri is varied which varies Ra for the problems. The domain Ω and boundary conditions are different for each test and will therefore be provided in the following subsections.

Let τ_h be a barycentric refined triangular mesh for Ω . We use $X_h = \mathbb{P}_2(\tau_h) \cap X$, $Q_h = \mathbb{P}_1^{disc}(\tau_h) \cap Q$, and $D_h = \mathbb{P}_2(\tau_h) \cap D$. We note that (X_h, Q_h) are LBB stable in this setting, and also provide

divergence free velocity solutions [1], so all the analysis of the previous sections applies. We also choose the initial guess to be $(u_0, p_0, T_0) = (0, 0, 0)$. Using the B-norm defined below, the convergence criteria will be given as

$$\|(u^k, T^k) - g_{PN}(u^k, T^k)\|_B := \sqrt{\nu \|\nabla(u^k - u^{k-1})\|^2 + \kappa \|\nabla(T^k - T^{k-1})\|^2} < 10^{-8},$$

and we use 200 iterations as the maximum number of allowed iterations. We also use AA in the Picard step of Picard-Newton in some tests cases to illustrate possible further improvements.

4.1 Differentially Heated Cavity

The first numerical test is the classical differentially heated cavity problem [3]. The domain is the unit square $\Omega = (0, 1)^2$, with boundary conditions

$$\begin{cases} u &= 0 \text{ on } \partial\Omega, \\ T(0, y) &= 0, \\ T(1, y) &= 1, \\ \nabla T \cdot n &= 0, \text{ on } x = 0, x = 1. \end{cases}$$

We use a mesh with max element diameter $h = 1/64$ and note that all results are comparable for other choices of h that we tested. Solutions to this system with $Ra = 10000$ are shown in figure 1.

We study the convergence of Picard-Newton for varying Ra . Convergence results are shown in figure 2 for $Ra = 50000, 100000, 150000, 200000,$ and 250000 . We observe that Picard-Newton converges for each Ra , and quadratic convergence is observed in the asymptotic range. As Ra increases, the number of iterations required for convergence increases as well. We observe the method remains stable even when it is (seemingly) not making progress in its residual.

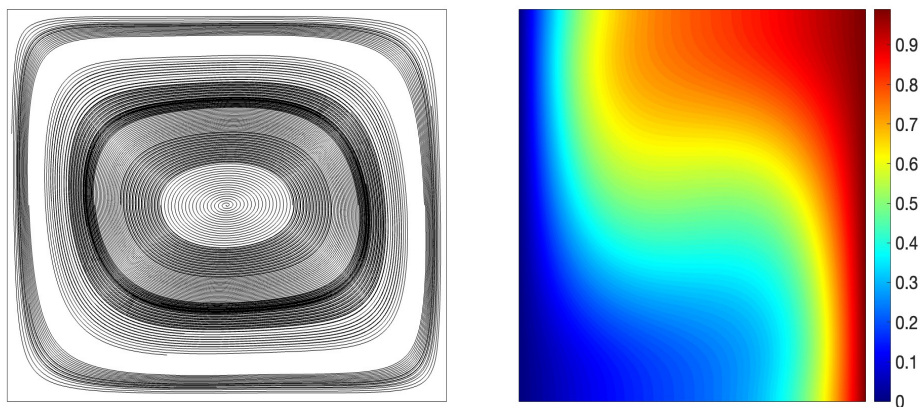


Figure 1: Shown above is the computed Boussinesq solution of the differentially heated cavity problem for velocity streamlines (left) and temperature contours (right) for $Ra = 10000$

For comparison, we also perform tests using Picard alone and Newton alone. In figure 3 (left) we see that Picard converges within 200 iterations for Ra up to 10000. For higher Ra , Picard does not

converge, but it does remain stable. Newton is able to converge for slightly higher Ra than Picard, as shown in figure 3 (left): it converges for up to $Ra = 15000$, but above this Ra we observe divergence. Moreover, as is typical for Newton, when it diverges, it blows up. The maximum Rayleigh number at which each method converges is given in table 4.1, and we observe that Picard-Newton is able to converge for Ra a full order of magnitude higher than Picard and Newton.

Method	Max Ra for convergence
Picard-Newton	250000
Picard	10000
Newton	15000

Table 2: Shown above is the maximum Ra (to the nearest 1000) at which each method converges.

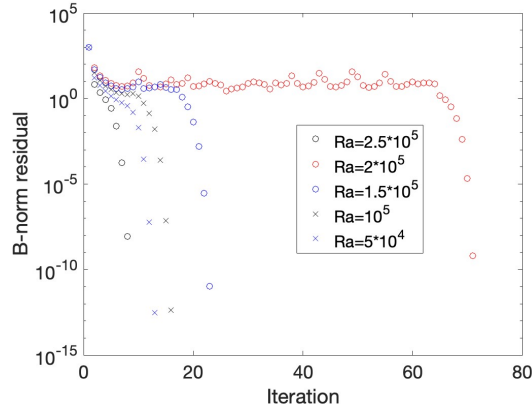


Figure 2: Shown above are convergence plots for Picard-Newton at varying Ra .

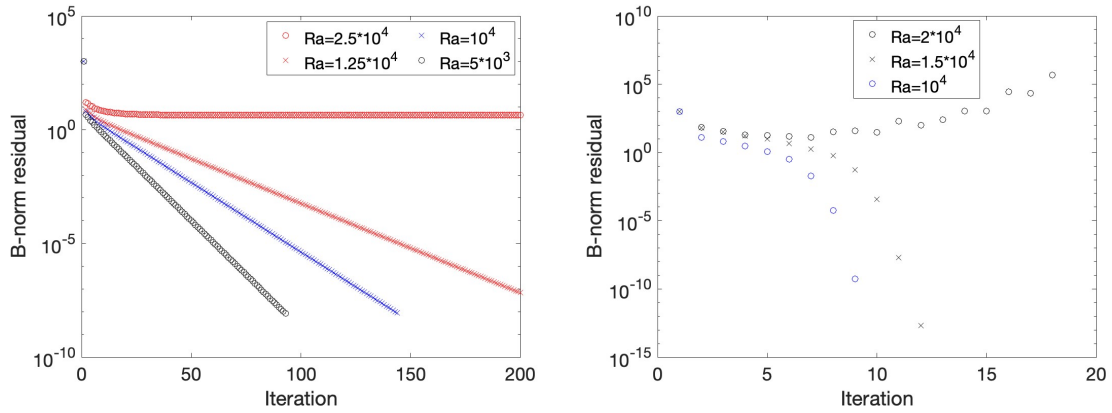


Figure 3: Shown above are convergence plots for Picard (left) and Newton(right) at varying Ra .

4.2 Boussinesq on a Complex Domain

The second numerical test is on a more complex domain shown in figure 4, with boundary conditions

$$\begin{cases} u &= 0 \text{ on } \partial\Omega, \\ T(x, 1) &= 1, \\ T(x, 0) &= \frac{2x}{7}, \\ \nabla T \cdot n &= 0 \quad 0 < y < 1. \end{cases}$$

Solutions for u and T shown on the domain in figure 4 for $Ra = 1000$. We use a Delaunay mesh with max element diameter $h = 7/64$, and again note that all results are comparable for other mesh sizes that we tested.

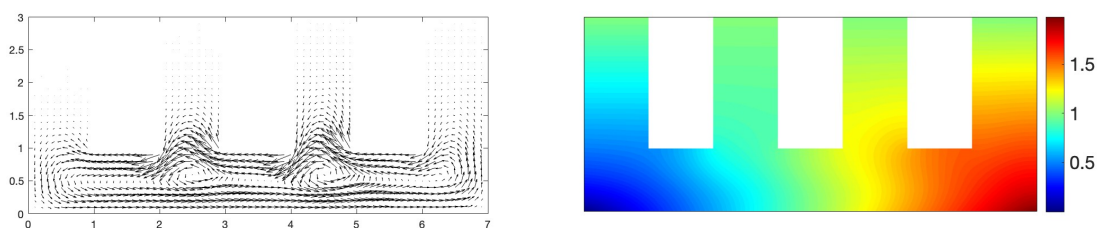


Figure 4: Shown above is the computed Boussinesq solution for u (left) and T (right) for $Ra = 1000$ in the second numerical test.

Convergence results for Picard-Newton are shown in figure 5, for $Ra = 5000, 10000, 15000, 20000, 25000,$ and 50000 . As in the previous test problem, we observe quadratic convergence for each Ra which Picard-Newton converges, for (up to $Ra = 10000$). For $Ra > 10000$, we do not observe convergence within 200 iterations but note the computed solutions remains stable.

Again for comparison, we solve the test problem using both Picard alone and Newton alone, and display their convergence results in figure 6. We see that Picard converges linearly for Ra up to 1000. For higher Ra , Picard does not converge but remains stable. Newton, in figure 6 (left), converges for Ra up to 2500 which is slightly higher than Picard. For $Ra = 5000$, convergence is not achieved but Newton curiously remains stable. For $Ra > 5000$ we see divergence, and solutions blow up. In comparison, using Picard-Newton we get convergence for $Ra = 20000$ with solutions that remain stable for all Ra that we tested.

Method	Max Ra for convergence
Picard-Newton	20000
Picard	1000
Newton	5000

Table 3: Shown above is the maximum Ra (to the nearest 100) at which each method converges.

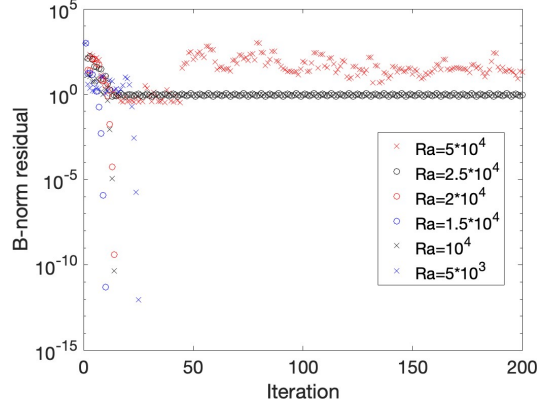


Figure 5: Shown above are convergence plots for Picard-Newton at varying Ra .

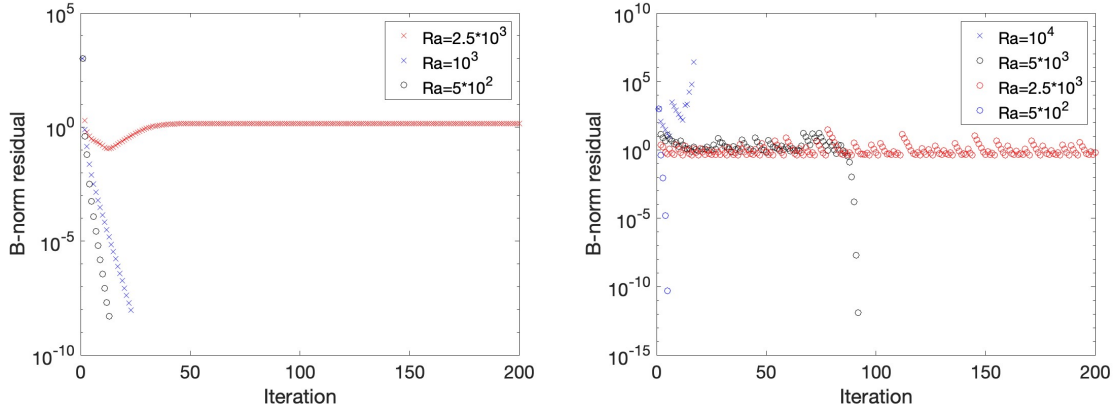


Figure 6: Shown above are convergence plots for Picard (left) and Newton (right) at varying Ra .

4.3 AAPicard-Newton

Anderson Acceleration (AA) is an extrapolation technique which utilizes previously computed iterates to construct the next solution. It is known to improve convergence for linearly convergent fixed point iterations like Picard [19, 7, 17, 22, 10, 7, 20]. Therefore, it is a natural addition to the Picard step of Picard-Newton and we call this iteration AAPicard-Newton.

4.3.1 Anderson-Acceleration

AA is defined as follows [19]. Let $g : Y \rightarrow Y$ be a fixed point operator for a Hilbert space Y .

Algorithm 4.1. AA for depth $m \geq 0$

Step 0: Choose $x_0 \in Y$

Step 1: Find $w_1 \in Y$ such that $w_1 = g(x_0) - x_0$. Set $x_1 = x_0 + w_1$.

Step k: For $k = 2, 3, \dots$. Set $m_k = \min\{k - 1, m\}$.

[a.] Find $w_k = g(x_{k-1}) - x_{k-1}$.

[b.] Solve the minimization problem for $\{\alpha_j^k\}_{k-m_k}^{k-1}$

$$\min \left\| \left(1 - \sum_{j=k-m_k}^{k-1} \alpha_j^k \right) w_k + \sum_{j=k-m_k}^{k-1} \alpha_j^k w_j \right\|_Y.$$

[c.] Set

$$x_k = \left(1 - \sum_{j=k-m_k}^{k-1} \alpha_j^k \right) (x_{k-1} + w_k) + \sum_{j=k-m_k}^{k-1} \alpha_j^k \alpha_j^k (x_{j-1} + w_j)$$

where $w_j = g(x_{j-1}) - x_{j-1}$ may be referred to as the update step or also as the nonlinear residual. Setting $m = 0$ returns the original fixed point iteration.

4.3.2 AAPicard-Newton for Differentially heated Cavity

We first apply AAPicard-Newton to the differentially heated cavity problem in section 4.1. Recall that for this problem Picard-Newton converges for Ra as high as 250000. Convergence for AAPicard-Newton, as shown in figure 7 for varying Ra and $m = 1$ (left) and $m = 3$ (right). AAPicard-Newton shows significant improvement in convergence for higher Ra both in iteration count and solvability. Convergence is even further improved with increased depth: for $m = 1$ we observe convergence up to $Ra = 500000$ and with $m = 3$ convergence is obtained up to $Ra = 750000$ (and convergence is accelerated by $m = 3$ over $m = 1$ for Ra where $m = 1$ converges).

Method	Max Ra for convergence
AAPicard-Newton: m=3	750000
AAPicard-Newton: m=1	500000
Picard-Newton	250000
Picard	10000
Newton	15000

Table 4: Shown above is the maximum Ra (to the nearest 1000) for which each method converges.

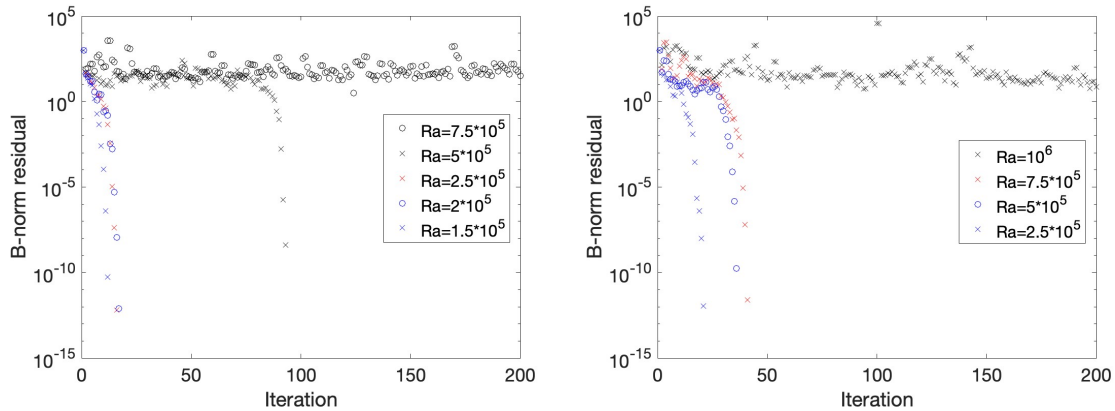


Figure 7: Convergence plots for AAPicard-Newton with $m = 1$ (left) and $m = 3$ (right) at varying Ra .

4.3.3 AAPicard-Newton on a Complex Domain

We next apply AAPicard-Newton to the heated cavity problem on a complex domain from section 4.2. Recall that for this problem Picard-Newton converges in 200 iterations for Ra up to 10000. AAPicard-Newton achieves convergence with depth $m = 1$ for Ra up to 125000 as shown in figure 8. This is further improved with depth $m = 3$ where AAPicard-Newton converges for Ra up to 75000. As before, for higher Ra we see stability for the method and it may converge if allowed to continue past 200 iterations.

Method	Max Ra for convergence
AAPicard-Newton: $m=3$	75000
AAPicard-Newton: $m=1$	125000
Picard-Newton	20000
Picard	1000
Newton	5000

Table 5: Shown above is the maximum Ra (to the nearest 100) for which each method converges.

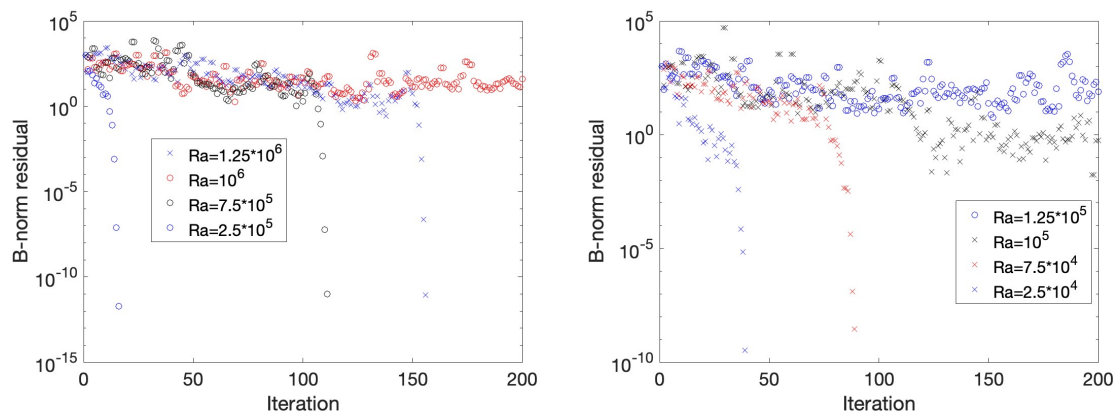


Figure 8: Shown above are convergence plots for AAPicard-Newton convergence with $m = 1$ (left) and $m = 3$ (right) at varying Ra .

5 Conclusion

The Picard-Newton iteration for the Boussinesq equations is an improvement upon the Newton iteration that provides less restrictive (sufficient) conditions for quadratic convergence. The sufficient conditions of Picard-Newton incorporate the accuracy bounds of the Picard step, which leads to a scaling of the sufficient conditions of Newton by a constant less than 1. Furthermore, the sufficient conditions of Picard-Newton depend solely upon the fluid velocity u^k due to the Picard step causing accuracy of T^k to depend on u^k . This is in stark contrast to the usual Newton whose sufficient conditions depends upon both u^k and T^k . Furthermore, Picard-Newton is stable for any Ra and any initial guess.

These behaviors are reflected in the numerical tests where for a simple domain we see convergence for high Ra and errors that remain stable. In comparison, Newton diverges for relatively low Ra

and Picard converges slower for the same Ra . This is further shown in the Boussinesq equations on a complex domain which is comparatively harder. Picard-Newton converges for high Ra and is stable, while Picard and Newton either converges slower or fail to converge for these same Ra .

Lastly, with the popularity of AA, linearly convergent methods like Picard are becoming faster and more applicable to problems where it is usually slow (or unable) to converge. This beneficial effect carries over to Picard-Newton: AAPicard-Newton improved Picard-Newton by lowering the iteration count for which the method converges for Ra , and also allows convergence for higher Ra .

6 Acknowledgements

All authors were partially supported by NSF grant DMS 2011490.

The author thanks Professor Leo Rebholz for helpful discussions regarding this work.

References

- [1] D. Arnold and J. Qin. Quadratic velocity/linear pressure Stokes elements. In R. Vichnevetsky, D. Knight, and G. Richter, editors, *Advances in Computer Methods for Partial Differential Equations VII*, pages 28–34. IMACS, 1992.
- [2] M. Benzi and M. Olshanskii. An augmented Lagrangian-based approach to the Oseen problem. *SIAM J. Sci. Comput.*, 28:2095–2113, 2006.
- [3] J. Boland and W. Layton. Error analysis for finite elements for steady natural convection problems. *Numerical Functional Analysis and Optimization*, 11:449–483, 1990.
- [4] S. Börm and S. Le Borne. \mathcal{H} -LU factorization in preconditioners for augmented Lagrangian and grad-div stabilized saddle point systems. *International Journal for Numerical Methods in Fluids*, 68:83–98, 2012.
- [5] X. Cai and D. Keyes. Nonlinearly preconditioned inexact Newton algorithms. *SIAM Journal on Scientific Computing*, 24, 2002.
- [6] H. Elman, D. Silvester, and A. Wathen. *Finite Elements and Fast Iterative Solvers with applications in incompressible fluid dynamics*. Numerical Mathematics and Scientific Computation. Oxford University Press, Oxford, 2014.
- [7] C. Evans, S. Pollock, L. Rebholz, and M. Xiao. A proof that Anderson acceleration improves the convergence rate in linearly converging fixed-point methods (but not in those converging quadratically). *SIAM Journal on Numerical Analysis*, 58:788–810, 2020.
- [8] T. Heister and G. Rapin. Efficient augmented Lagrangian-type preconditioning for the Oseen problem using grad-div stabilization. *Int. J. Numer. Meth. Fluids*, 71:118–134, 2013.
- [9] K. Huang, B. Mohanty, F. Leij, and M. Genuchten. Solution of the nonlinear transport equation using modified Picard iteration. *Advances in Water Resources*, 21:237–249, 1996.
- [10] C.T. Kelley. *Solving Nonlinear Equations with Newton’s Method*. SIAM, Philadelphia, 2003.
- [11] W. Layton. *An Introduction to the Numerical Analysis of Viscous Incompressible Flows*. SIAM, Philadelphia, 2008.
- [12] L. Liu, F. Hwang, L. Luo, X. Cai, and D. Keyes. A nonlinear elimination preconditioned inexact Newton algorithm. *SIAM Journal on Scientific Computing*, 44, 2022.

- [13] L. Liu and D. Keyes. Convergence analysis for the multiplicative schwarz preconditioned inexact Newton algorithm. *SIAM Journal on Scientific Computing*, 54, 2016.
- [14] K. Lust, D. Roose, A. Spence, and A. Champneys. An adaptive Newton-Picard algorithm with subspace iteration for computing periodic solutions. *SIAM Journal on Scientific Computing*, 19:1188–1209, 1998.
- [15] S. Mehl. Use of Picard and Newton iteration for solving nonlinear ground water flow equations. *Groundwater*, 44:583–594, 2006.
- [16] C. Paniconi and M. Putti. A comparison of Picard and Newton iteration in the numerical solution of multidimensional variably saturated flow problems. *Water Resources Research*, 30(12):3357–3374, 1994.
- [17] S. Pollock and L. Rebholz. Anderson acceleration for contractive and noncontractive operators. *IMA Journal of Numerical Analysis*, 41(4):2841–2872, 2021.
- [18] S. Pollock, L. Rebholz, X. Tu, and M. Xiao. Analysis of the Picard-Newton iteration for the Navier-Stokes equations: global stability and quadratic convergence. *Submitted*, 2024.
- [19] S. Pollock, L. Rebholz, and M. Xiao. Anderson-accelerated convergence of Picard iterations for incompressible Navier-Stokes equations. *SIAM Journal on Numerical Analysis*, 57:615–637, 2019.
- [20] S. Pollock, L. Rebholz, and M. Xiao. Anderson-accelerated convergence of Picard iterations for incompressible Navier-Stokes equations. *SIAM Journal on Numerical Analysis*, 57(2):615–637, 2019.
- [21] A. Potschka, M. Mommer, J. Schloder, and H. Bock. Newton-Picard-based preconditioning for linear-quadratic optimization problems with time-periodic parabolic PDE constraints. *SIAM Journal on Scientific Computing*, 34:A1214–A1239, 2012.
- [22] A. Toth and C.T. Kelley. Convergence analysis for Anderson acceleration. *SIAM Journal on Numerical Analysis*, 53(2):805–819, 2015.
- [23] J. Zhang. A relaxed Newton-Picard like method for Huber variant of total variation based image restoration. *Computers and Mathematics with Applications*, 78(1):224–239, 2019.
- [24] T. Zhong, J. Yuan, and Z. Shi. Decoupled two grid finite element method for the time dependent natural convection problem I: spatial discretization. *Numerical Methods for Partial Differential Equations*, 31:2135–2168, 2015.